Physica 134B (1985) 480-486
North-Holland, Amsterdam

HOT ELECTRON SPECTROSCOPY OF GaAs

A.F.J. LEVI
AT&T Bell Laboratories, 600 Mountain Avenue, Murray Hill, NJ 07974, USA

J.R. HAYES
Bell Communications Research, 600 Mountain Avenue, Murray Hill, NJ 07974, USA

P.M. PLATZMAN and W. WIEGMANN
AT&T Bell Laboratories, 600 Mountain Avenue, Murray Hill, NJ 07974, USA

We report results both experimental and theoretical on the dynamics of hot electron transport in GaAs. Total elastic and inelastic scattering rates are calculated and compared with the results of a new experimental technique "Hot Electron Spectroscopy". The magnetic field dependence of hot electron spectra has been studied. It is shown that application of a magnetic field normal to the injection direction has a dramatic effect on the spectra whereas a magnetic field applied parallel to the injection direction has no effect. The magnetic field is shown to increase the effective transit region width of the spectrometer enabling us to obtain a scattering rate for hot electrons. The experimentally determined rate gives good agreement with a theoretically determined rate considering scattering by coupled plasmon/phonon modes.

Hot electron transport is of both fundamental and technological importance. Historically, the high field transport measurements of Shockley and Ryder[1], the Gunn effect[2] and the luminescence studies of Shah and Leite[3] were all examples of hot electron effects in semiconductors. However, none of this pioneering work gave direct spectroscopic information on the behavior of hot electrons in solids. Today, with ever decreasing device dimensions it is more important than ever to understand the behavior of hot electrons in small scale structures. Infact, until recently, an understanding of hot electron effects in semiconductors has been limited by a lack of experimental data with which to compare theoretical predictions. The introduction of a new technique "Hot Electron Spectroscopy"[4] has changed this situation. Using this technique one may now obtain direct spectroscopic information on the dynamics of non-equilibrium carriers in semiconductors.

The experimental method, described in detail, in reference 5, uses the unique degree of control currently available with Molecular Beam Epitaxy (MBE) to form two bulk triangular potential barriers in the conduction band of a single crystal of GaAs. In the structure described here we have incorporated two bulk triangular potential barriers separated by a region of n^+ (Si-impurity) GaAs. The bulk triangular barriers were formed by placing a thin p^+ (Be-impurity) layer in a region of low carrier concentration bounded by n^+ layers.[6] The grown epilayers were fabricated into a two level mesa structure using standard chemical etching techniques to reveal the three n^+ layers. Ohmic contacts were made to the layers by rapidly thermally annealing an evaporated Au-Sn alloy.

A schematic cross section of the fabricated two level mesa structure together with a diagram of the conduction band edge is shown in Figs. 1(a) and (b) respectively. The voltages applied to and the currents flowing in this structure are best described using standard transistor notation where the emitter, base and collector are indicated in Fig. 1.

0378-4363/85/$03.30

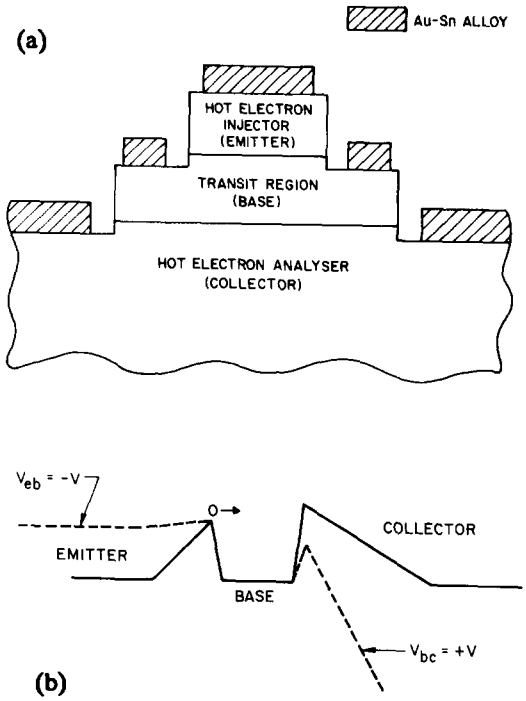

Figure 1. Schematic diagram of the MBE-grown GaAs epilayers comprising the two level mesa structure are shown in (a) together with a schematic of the conduction band edge of the hot electron injector (emitter), transit region (base) and hot electron analyser (collector) in (b). The broken lines indicate the conduction band edge of the structure when biased.

In order to acquire a hot electron spectrum the following procedure was adopted. With the transit region (base) at ground potential, a negative bias ($-V_{eb}$) was applied to the emitter so that a nearly mono-energetic beam of electrons was injected into the transit region. The emitter-base triangular potential barrier therefore formed the "hot electron injector" injecting a narrrow cone in the forward direction, normal to the plane of the barriers. The injected electrons were scattered in the transit region and the resulting distribution at the far edge of the transit region was analysed using the collector as a "hot electron analyser". The analyser works by applying a positive bias, V_{bc}, to the collector with respect to the transit region. This has the effect of lowering the barrier energy, ϕ_{bc}, enabling spectroscopic information on the electron distribution to be obtained. It was shown in reference 5 that the analyser current j_c is given by

$$j_c = -\frac{e}{m_e}\int_{p_\perp^0}^{\infty} p_\perp n(p_\perp)dp_\perp \qquad (1)$$

which enables one to show that

$$\frac{dj_c}{dV_{bc}} \propto n(p_\perp^0) \qquad (2)$$

where j_c is the collected current, $n(p_\perp^0)$ is the distribution of hot electron momentum normal to the plane of the triangular barriers, $p_\perp^0 = \sqrt{2m_e\phi_{bc}}$, e is the electronic charge and m_e is the effective electron mass. In this way, measuring dj_c/dV_{bc} as a function of the base/collector bias, one obtains detailed spectroscopic information on scattering mechanisms in the transit region.

Figure 2 shows the results of electrical measurements peformed at 4.2K on samples having an injection energy of 0.25 eV and an n^+ transit region (base) carrier concentration of $1\times10^{18}cm^{-3}$. The hot electron spectra for two samples of base width 1200Å and 1700Å are shown in Fig. 2a and Fig. 2b respectively for four different emitter currents, I_e.

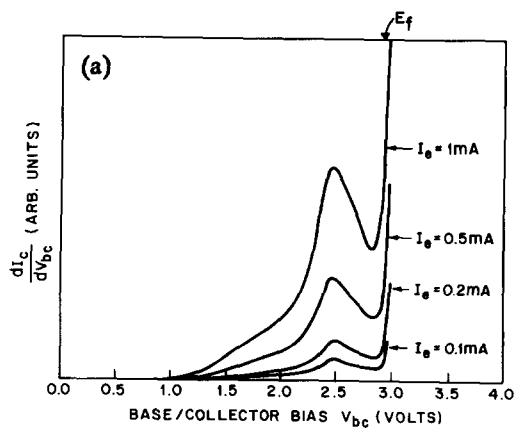

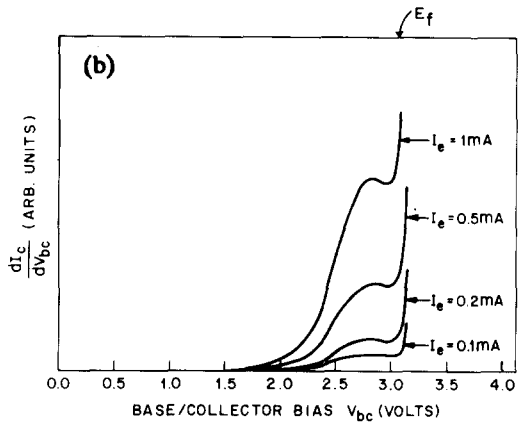

Figure 2. (a) Hot electron spectra obtained for a sample having a 1200Å transit region. (b) Hot electron spectra obtained for a sample having a 1700Å transit region. The positions of the Fermi energy E_F are indicated.

There is a theshold for current collection at around 1.0V since no electrons can be collected when $\phi_{bc} > \phi_{eb}$. Between 1.0 and 3.0V the collected current is due to the hot electrons that have traversed the collector barrier. At around 3.0V bias ϕ_{bc} is so small that thermally excited electrons in the n^+ transit region can be collected; dominating the collected current (j_c). In order to obtain the correct hot electron spectrum it is necessary to subtract this background contribution from the data.

As a preliminary to discussing these results it should be noted that if no scattering occurred in the transit region one would expect to see a narrow peak at around 1.0V. In contrast both samples show a rather broad distribution peaking close to the Fermi energy E_F, indicating that electrons have experienced significant scattering during transit. The sample with the 1200Å transit region shows a pronounced peak further from E_F than the sample with the 1700Å transit region; indicating that electrons have experienced fewer collisions. In both samples it is obvious that the injected electrons have undergone significant momentum change. It is also clear from the shape of the spectrum that the electrons cannot be assigned a hot electron temperature as they do not have a Maxwellian distribution.

We now describe the effects that a magnetic field applied perpendicular to the direction of electron injection ($B_\perp$) has on hot electron spectra. The simplest description of hot electron transport utilizes a classical kinematical model in which an electron injected into the transit region, prior to the application of a magnetic field, has a straight trajectory between scattering events. However, when a magnetic field is applied this trajectory is modified, the electron describes part of a circular orbit between collisions, the radius of which, r, is given by

$$r = \frac{p\,c}{B_\perp e} \tag{3}$$

where p is the electron's momentum, e its charge, c the velocity of light and $B_\perp$ the applied magnetic field.

To understand the effect of the magnetic field consider what would happen to an electron transiting from the injector to the analyser without a collision, i.e., a ballistic electron. A hot electron injected into the transit region with all its momentum, $p = \sqrt{2m_e\phi_{bc}}$, in the forward direction is analysed after traversing, d, the transit region width. When $B_\perp$ is applied to the sample two effects occur that influence the collection of the injected electron. Firstly the electron trajectory is increased from d to d' and hence the probability that an electron be scattered is increased and secondly, although the magnitude of the momentum that the ballistic electron has when it arrives at the analyser barrier is the same, because of the imposed circular orbit, it now has both a component normal to and parallel with the plane of the analyser barrier. The analyser barrier, being only sensitive to normal component of momentum, collects the electron at a lower barrier energy. This qualitative description of ballistic electron transport in a magnetic field may be applied in a natural way to the case of

non-ballistic, hot electron, transport.

The measured magnetic field dependence of the specta shown in Fig. 2a (transit region width 1200Å, injection energy 0.25eV) is shown in Fig. 3 for fields up to 4.5×10^4 Gauss.

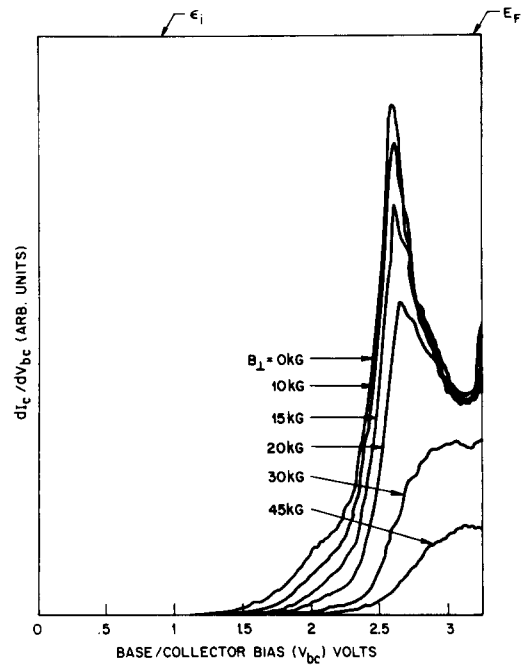

Figure 3. Magnetic field dependence of a hot electron spectrum shown in Fig. 2a. The magnetic field is applied perpendicular to the direction of current flow at the hot electron injector (emitter). The injection energy ϵ_i and the position of the Fermi energy E_F is indicated for this particular sample having a transit region width of 1200Å.

The magnetic field $B_\perp$ was applied perpendicular to the direction of electron injection. This study was undertaken for two reasons, firstly to measure changes in a given spectrum with applied $B_\perp$ to establish that hot electron effects were indeed being observed and secondly to measure the changes in a given spectrum and thereby infer a scattering rate for hot electrons. With $B_\perp = 0$ there are two outstanding features of the spectrum that should be pointed out, the pronounced peak close to the Fermi energy and the shoulder at higher barrier energies. Both features are dramatically altered by the application of a magnetic field, the shoulder disappears and the peak merges with the Fermi energy at 4.5×10^4 Gauss. For clarity the variation of three points on the barrier (1.5, 2.0, 2.5 Volts) are shown in Fig. 4.

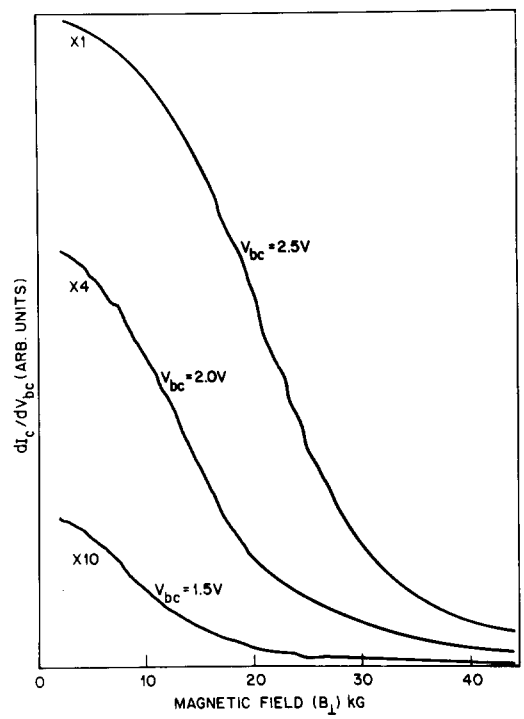

Figure 4. Variation of spectral intensity with applied magnetic field for three indicated hot electron analyser (collector) biases.

It is possible to infer a hot electron scattering rate from the magnetic field dependence using two reasonable assumptions; namely that electrons scattered due to an increase in effective transit region width lose sufficient energy that they no longer contribute to the collection current at a given analyser barrier energy and that the change in perpendicular momentum of the electrons not scattered is given by the cross product of the magnetic field and

the velocity. Using these assumptions we have obtained a scattering rate from the variation of the spectra at 1.5 Volts analyser bias (Fig. 4) for hot electrons of $2-3\times10^{13}$ s^{-1}.

It is interesting to note that application of a 3×10^4 Gauss magnetic field allows one to reproduce the spectra of a sample having a transit region width of 1700Å. However, application of a magnetic field in a direction parallel to the electron motion shows no change in the spectra. This of course is not surprising since, in this case, we expect injected electrons to follow a helical path between collisions so that the effective path length between injector and analyser remains unchanged.

In order to understand the non-equilibrium behavior of hot electrons in GaAs we must first consider the problem of scattering a hot electron from an extremely thin "sample" of doped material. As long as the energy of the hot electron is not too low and the percentage of scattered electrons from our hypothetical sample is small, we may treat such scattering in the Born approximation. In the more complicated case of a thick sample, multiple scattering effects must be taken into account either by a Monte-Carlo type calculation or some other procedure. In this paper we will present the simple scattering results for realistic values of the parameters (incoming electron energy, Fermi energy, phonon frequency etc.)

We first write the differential rate, $dR_{inelastic}$, for inelastically scattering hot electrons off the Fermi sea. The incoming mono-energetic beam of electrons having a momentum $\hbar k_i$ and energy $E_i = \hbar^2 k_i^2/2m_e$ are scattered into a new state having momentum $\hbar k_f$ and energy $E_f = \hbar^2 k_i^2/2m_e$. When the incoming electron is scattered it loses energy $\hbar\omega$ and is scattered by an angle θ, changing momentum by $\hbar q$. Since the injected electrons have an energy significantly greater than E_F we can, as a first approximation, neglect exchange effects and treat the scattering in the Born approximation. In the case the inelastic differential rate is given by[7]

$$dR_{inelastic} = \frac{8\pi e^2}{\hbar q^2} S(q,\omega) \frac{d^3q}{(2\pi)^3} \tag{4}$$

where

$$S(q,\omega) = -\mathrm{Im}\frac{1}{\epsilon(q,\omega)} \tag{5}$$

The frequency and wavevector dependent dielectric function $\epsilon(q,\omega)$ may be written as

$$\epsilon(q,\omega) = \epsilon_\infty \left(\frac{\omega^2-\omega_{LO}^2}{\omega^2-\omega_{TO}^2}\right) + \chi(q,\omega) \tag{6}$$

where ω_{LO} and ω_{TO} are the longitudinal and transverse optical phonon frequencies respectively and ϵ_∞ is the high frequency dielectric constant. The first term in equation 6 is the long wavelength phonon contribution and the second term, $\chi(q,\omega)$ comes from the conduction electrons. We are justified in using the long wavelength limit for the phonons since its dielectric function varies on a scale set by a reciprocal lattice vector k_L and in our case the momentum change q for inelastically scattered hot electrons in such that $q \ll k_L$.

In general $\chi(q,\omega)$ cannot be calculated exactly. However, because the carrier concentration of electrons in the transit region is high ($n = 1\times10^{18}$ cm^{-8}) and the effective electron mass is low ($m_e = 0.07\ m_0$) Coulomb interactions among electrons are weak i.e., $r_s \equiv (3/4\pi m)^{1/3}(m_e e^2/\hbar^2\epsilon_\infty) \cong 0.7$. In this case we can assume the non-interacting form of $\chi(q,\omega)$: $\chi_o(q,\omega)$ where

$$\chi_o(q,\omega) = \frac{\xi}{x^3}\left[2x + \left(1-1/4\left(x-\frac{y}{x}\right)^2\right)\ln\left\{\frac{y-x(x+2)}{y-x(x-2)}\right\} + \left(1-1/4\left(x+\frac{y}{x}\right)^2\right)\ln\left\{\frac{-y-x(x+2)}{-y-x(x-2)}\right\}\right] \tag{7}$$

in which $\xi = \frac{m_e}{2}\left(\frac{e}{\pi\hbar}\right)^2\left(\frac{8\pi}{3n}\right)^{1/3}$, $x = q/k_F$ and $y = \hbar\omega/E_F$. This gives for the loss function, $S_o(q,\omega)$,

$$S_o(q,\omega) = -\mathrm{Im}\,\frac{1}{\epsilon_\infty\left(\frac{\omega^2-\omega_{LO}^2}{\omega^2-\omega_{TO}^2}\right)+\chi_o(q,\omega)} \quad (8)$$

The relevant features of $S_o(q,\omega)$ are diagramed in Fig. 5 for GaAs having a carrier concentration of 1×10^{18} cm^{-3}.

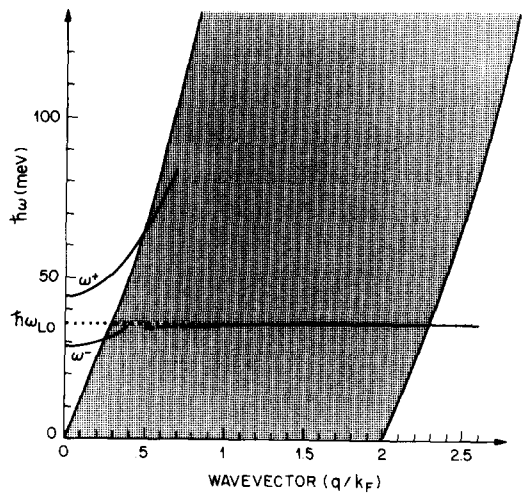

Figure 5. Dispersion of the coupled plasmon/phonon modes for a carrier density of $n=1\times10^{18}$ cm^{-3} in GaAs. Here we have used $\epsilon_\infty = 11.1$, $\hbar\omega_{LO} = 36.3$ meV, $\hbar\omega_{TO} = 33.3$ meV and $m_3 = 0.07\ m_0$. The dotted line indicates the bare LO phonon frequency and is not part of the coupled plasmon/phonon dispersion.

Because both the bare plasmon and optical phonon frequencies are similar they interact to form two coupled plasmon/phonon modes of frequency ω^+ and ω^- at q=0.[8] With increasing wavevector these modes exhibit dispersion and at some modest wavevector ($q/k_F \cong 0.3$) they enter the electron-hole continuum shown by the shaded region. Here the collective plasmon/phonon modes are Landau damped (dashed lines in Fig. 5) by the excitation of single electron hole pairs from the Fermi sea. In any given inelastic scattering event there will be a contribution from the coupled plasmon/phonon modes and from the continuum. At larger wavevectors only the dispersionless longitudinal optical phonon mode and the single particle continum exists.

In Fig. 6 we have plotted the total inelastic scattering rate $1/\tau$, as a function of the incoming hot electron energy measured from the bottom of the conduction band for several different carrier densities in GaAs. We note that our definition of total inelastic scattering rate does not weight $1/\tau$ with the energy loss. As can be seen the scattering rates are, as expected, zero below the Fermi energy for a finite carrier concentration and zero below $\hbar\omega_{LO}$ for n=0. Since the scattering rate is weighted towards the forward direction (small q, see equation 4) we find that the total rate shows a mild threshold at ω^+ and ω^-. In addition, results obtained for n=0 agree with the values given by Conwell[9] for phonon emission.

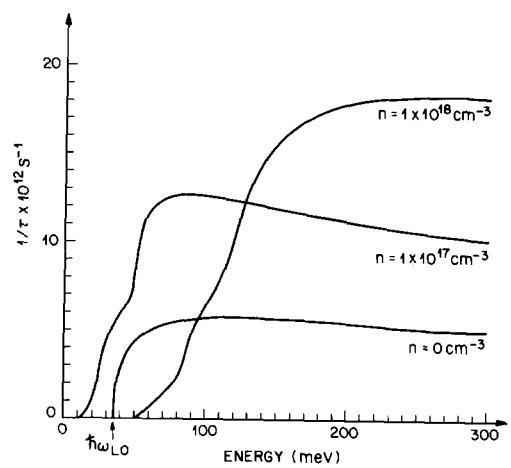

Figure 6. Total inelastic electron scattering rate as a function of hot electron energy measured from the bottom of the conduction band for different carrier densities in GaAs.

At a density $n = 1\times10^{18}$ cm^{-3} the inelastic scattering rate increases, attaining a maximum value of

approximately 2×10^{13} s^{-1} at incident electron energies of around 250 meV. This is in reasonable agreement with the rates deduced from the measured dependence of the spectra with applied magnetic field. Given that the velocity of such an electron is 1×10^{8} cm s^{-1} we obtain a mean free path of 500Å. At greater incident electron energies the rate decreases. This energy dependence occurs because, for large E_i, $\hbar^2q^2 \cong 8m_e E_i \sin^2(\theta/2)$ so that the $1/q^2$ factor in equation 1 leads to a $1/E_i$ decrease of the scattering rate. However, at incident electron energies greater than 300 meV complications associated with intervalley scattering and with details of Bloch wavefunctions arise because of the subsidiary L minimum[10] in GaAs. We therefore restrict our attention to energies below 300 meV.

There is an additional elastic contribution to the scattering rate from ionized impurities which must be considered. The elastic scattering is specified by the momentum transfer $q = 2k_i \sin(\theta/2)$ where θ is the scattering angle. For the case of weak elastic scattering (Born approximation) the differential rate is given by

$$dR_{elastic} = \frac{2\pi n_i m_e e^4}{\hbar^3 k_i^3} \frac{\eta d\eta}{\left(\eta^2 \epsilon(2k_i\eta,0)\right)^2} \qquad (9)$$

where n_i is the density of ionized impurities (n_i=n) and $\eta \equiv \sin(\theta/2)$. Equation 9 corresponds to scattering from donor ions screened by the conduction electrons. An evaluation of the total rate gives, for an electron density $n=1\times10^{18}$ cm^{-3} and a hot electron energy E_i=250 meV, a mean free path of around 1300Å.

We note that our definition of total elastic scattering rate does not weight the rate with scattering angle. However, the major contribution to the elastic rate comes from small angle scattering (average scattering angle $\theta_{av} < 20°$ for $E_i = 250$ meV). We therefore conclude that elastic scattering at these densities does not play a dominant role, the mean free path of hot electrons essentially being determined by inelastic scattering events.

In conclusion, we have developed a theory of injected hot electron transport in GaAs which indicates that inelastic electron scattering dominates the transport process at the carrier concentrations of interest. Application of a magnetic field has enabled us to draw a two important conclusions. First, the magnetic field dependence of the observed spectra is strong evidence that hot electron transport is being measured. Second, the spectra change in a predictable way, enabling us to infer scattering rates for hot electrons in GaAs which are in reasonable agreement with theoretical predictions.

We wish to thank S. J. Allen, S. L. McCall and H. L. Störmer for useful discussions and T. Uchida for technical assistance.

REFERENCES

1. W. Shockley, Bell System Tech. J., *30*, 990 (1951)
2. J. B. Gunn, Solid State Commun., *1*, 88 (1963)
3. J. Shah and R. C. C. Leite, Phys. Rev. Lett., *22*, 1304 (1969)
4. J. R. Hayes, A. F. J. Levi and W. Weigmann, Elect. Lett., *20*, 851 (1984)
5. J. R. Hayes, A. F. J. Levi and W. Weigmann, Phys. Rev. Lett., *54*, 1570 (1985).
6. R. J. Malik, K. Board, C. E. C. Wood, L. F. Eastman, T. R. AuCoin and R. L. Ross, Elect. Lett., *16*, 837 (1980).
7. D. Pines and P. Nozieres, "The Theory of Quantum Liquids" Benjamin (1966).
8. M. E. Kim, A. Das and S. D. Senturia, Phys. Rev., *B18*, 6890 (1978).
9. E. M. Conwell, "High Field Transport in Semiconductors" Solid State Physics; Advances in Research and Applications Eds. H. Ehrenreich, F. Seitz and D. Turnbull. Vol. 9 Academic Press (1967).
10. H. C. Casey and M. B. Panish, "Heterostructure Lasers, Part A: Fundamental Principles," p. 193 Academic Press (1978).